Journal of Photochemistry & Photobiology A: Chemistry 361 (2018) 105–111

Contents lists available at ScienceDirect

Journal of Photochemistry & Photobiology A: Chemistry

journal homepage: www.elsevier.com/locate/jphotochem

Atmospheric degradation of *n*-butyl formate in the presence of O_2 and NO_2

Jesús A. Vila, Gustavo A. Argüello, Fabio E. Malanca*

INFIQC (CONICET), Departamento de Fisicoquímica, Facultad de Ciencias Químicas, Universidad Nacional de Córdoba, Ciudad Universitaria, X5000HUA Córdoba, Argentina

ARTICLE INFO

Keywords:
Peroxynitrate
Atmospheric degradation
Butyl formate
Peroxy butyl formyl nitrate

ABSTRACT

The mechanism for the chlorine initiated oxidation reaction of *n*-butyl formate has been determined in the presence and absence of NO_2. Chlorine atoms initiate the oxidation at five different sites of the molecule, leading to the formation of carbonylic and dicarbonilic species, nitrates, and a new peroxynitrate. The detailed list includes HC(O)OH, $CH_3CH_2C(O)H$, $CH_3CH_2CH_2C(O)H$, $HC(O)CH_2CH_2CH_2OC(O)H$, $CH_3C(O)CH_2CH_2OC(O)H$, $CH_3CH_2C(O)CH_2OC(O)H$, $CH_3CH_2CH_2C(O)OC(O)H$, $CH_3CH_2CH_2CH_2OC(O)OONO_2$, $CH_3CH_2CH_2CH_2ONO_2$, and $CH_3CH_2CH_2ONO_2$. The complete set of products is discussed and compared with those obtained from other formates. A comparison between experimental results and those obtained using SAR (Structure-Activity Relationship) methods was performed.

1. Introduction

The study of the photochemical degradation of volatile organic compounds (VOCs) emitted to the atmosphere is important because it allows us to understand the physicochemical processes that occur in the atmosphere and bring information about their degradation products. Esters are emitted from both antropogenic (flavorings and perfumes) and biogenic (fruits and vegetables) sources, and also formed by the degradation of alcohols and ethers.

Formates are volatile organic compounds, and due to their insecticidal, fungicidal, and pesticidal properties they are used for fumigation of dried fruit. Ethyl formate ($CH_3CH_2OC(O)H$, EF) is used in the fumigation of packages of dry fruits [1–4] and as potential disinfectant treatment for eucalyptus weevil in apples [5]. EF also could be formed in the photo-oxidation of diethyl ether with yields between 66 and 92% [6,7]. In addition, *n*-propyl formate ($CH_3CH_2CH_2OC(O)H$, nPF) is produced and emitted by many fruits and vegetables as a flavoring component [8].

The tropospheric reactivity of formates is mainly controlled by their reaction with OH radicals (the rate coefficient for reaction ranges from 1.8×10^{-13} to 3.7×10^{-12} $cm^3\,molec^{-1}\,s^{-1}$) since the reactions with nitrate radicals (k around 0.3–6 $\times 10^{-17}$ $cm^3\,molec^{-1}\,s^{-1}$), ozone or photolysis are slow processes [9–11].

Le Calvé et al. measured the temperature dependence for the rate coefficients of hydroxyl radicals with methyl, ethyl, *n*-propyl, and *n*-butyl formate; calculated their atmospheric lifetimes (66.9, 13.6, 6.4 and 3.3 days, respectively) and concluded that formates could be transported over large distances from their emission location [12].

Since then, there have been other studies on formates, but the need to determine the reaction mechanisms in gas phase is still of concern, particularly their reaction products in both clean (pristine) and polluted atmospheres. Notario et al. [13], Sellevág et al. [14], Wallington et al. [15], Ide et al. [16] and Zhang et al. [17] determined the rate constant of formates with chlorine atoms, while Wallington et al. [18], Malanca et al. [19], and Vila et al. [20] extended the studies to the determination of mechanisms of methyl, ethyl, and propyl formates, respectively. In an attempt to close the gap on the study of formates, we present in this paper the results on the photo-oxidation of *n*-butyl formate (nBF) (initiated by chlorine atoms) in the presence and absence of nitrogen dioxide.

2. Experimental section

2.1. Materials

Commercially available samples of *n*-butyl formate (Sigma Aldrich) and O_2 (AGA) were used. NO_2 was synthetized by thermal decomposition of $Pb(NO_3)_2$. Cl_2 was prepared by the reaction between HCl and $KMnO_4$, and was further distilled.

2.2. Procedure

Gases were manipulated in a glass vacuum line equipped with two capacitance pressure gauges (0–760 Torr, MKS Baratron; 0–70 mbar, Bell and Howell). Photolyses of mixtures of nBF (5.0 mbar)/Cl_2 (2.5 mbar)/NO_2 (0 to 2.0 mbar)/O_2 (1000 mbar) were carried out in an

* Corresponding author.
E-mail address: fmalanca@fcq.unc.edu.ar (F.E. Malanca).

https://doi.org/10.1016/j.jphotochem.2018.04.052
Received 23 January 2018; Received in revised form 26 April 2018; Accepted 29 April 2018

infrared gas cell (optical path 23.0 cm; silicon windows) using three black lamps (PHILIPS TL 8W BLB Model, 8 W, λ > 360 nm, length 30.2 cm) and the temporal variation of reactants and products was followed through infrared spectroscopy. Spectra were acquired in the range 4000–400 cm^{-1} with a resolution of 2 cm^{-1} using a Fourier Transform Infrared Spectrophotometer (FTIR, Bruker IFS28). This set-up was also used to quantify the products formed.

Additionally, to identify some of the products, samples were photolyzed in a 5 L glass flask and the resulting mixtures were collected in a cold trap to concentrate all products, which were then analyzed by gas chromatography/mass spectrometry (GC/MS) on a Shimadzu GC–MS-QP 5050 spectrometer equipped with a capillary column Zebron 2B-5MS (30 m × 0.25 mm × 0.25 μm) using helium as eluent at a flow rate of 1.1 mL/min. Both injector and ion source temperatures were 280 °C, the oven heating ramp was 15 °C/min from 25 °C up to 280 °C. The pressure in the MS instrument was 10^{-5} Torr, precluding ion-molecule reactions from taking place, and MS recordings were made in the electron impact (EI) mode with an ionization energy of 70 eV.

The ^{1}H NMR was used to identify the aldehydes formed as products of the photo-oxidation. The ^{1}H NMR (400.1 MHz) spectra were measured at 298 K on a Bruker Avance 400 spectrometer. The sample was dissolved (bubbled) in $CDCl_3$ in a 5 mm NMR tube provided with a PTFE valve.

To corroborate the identity of some products and to determine the relative importance of the main reaction paths of oxy radicals (RO·), theoretical calculations were performed using the Gaussian 09 program suite [21]. Geometric optimizations and calculations of the vibrational frequencies were carried out applying Density Functional Theory (DFT) methods, using the B3LYP exchange functional with 6-311 + + G(d,p) basis in much the way used by other authors to calculate theoretical spectra of similar molecules (e.g. 1-, 2-, 3-, and 4-oxobutylformates) and to obtain thermodynamical data in order to compare the relative importance of reaction path [22–24].

3. Results and discussion

3.1. Products identification and quantification in the presence and absence of NO_2

Fig. 1 shows the infrared spectra obtained in the photolysis of nBF/Cl_2/O_2 mixtures. The first and second traces correspond to the spectra obtained at t = 0 and t = 30 min of irradiation. It is clear that carbon dioxide (peak at 667 cm^{-1}) and formic acid (peaks at 1105 and 1775 cm^{-1}) are formed. The presence of formic acid could be corroborated by comparison to standard spectra like the one shown in the third trace. The fourth trace, obtained from the subtraction of nBF and formic acid to the second trace, shows the other photolysis products whose identities will be discussed later because their identification required bulk quantities that, in turn, required special experiments. For them, the photo-oxidation was generally performed in a 5 L photo-reactor and the resulting mixture was passed through cold traps in liquid nitrogen. The condensable fraction was then allowed to reach room temperature and was further analyzed by GC/MS. A typical chromatogram shows the following peaks (retention time, min): 2.08, 2.56, 4.33, 5.20, 5.60. The first three peaks correspond to formic acid, butanal, and nBF, respectively. The remnant peaks were assigned, based on their fragmentation patterns, to $CH_3C(O)CH_2CH_2OC(O)H$ (*m/e*: 15, CH_3^+; 43, CH_3CO^+; 45, CHO_2^+; 55, $C_3H_3O^+$; 72, $C_2O_3^+$; 87, $C_4H_7O_2^+$;102, M- CH_3; 115, M^+) and $CH_3CH_2C(O)CH_2OC(O)H$ (*m/e*: 27, $C_2H_3^+$; 29, $C_2H_5^+$, CHO^+; 45, CO_2H^+; 55, $C_3H_3O^+$; 57, $CH_3CH_2C(O)^+$; 59, $C_3H_7O^+$; 72, $C_4H_8O^+$; 87, $C_4H_7O_2^+$; 101, M–CH_3; 115 M^+).

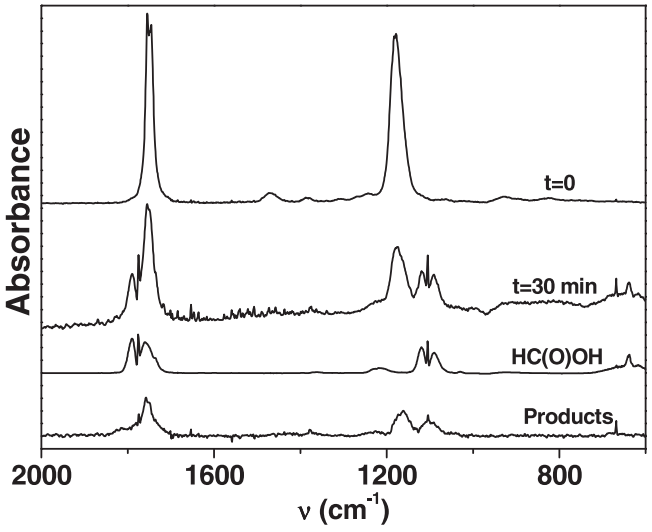

Fig. 1. Photo-oxidation of *n*-butyl formate in the absence of NO_2. Traces from top to bottom: before irradiation; after 30 min photolysis; reference spectrum of formic acid; result of subtracting *n*-butyl formate and formic acid from second trace.

A further proof of their identity required the help of other techniques. The GAUSSIAN 09 package was used to simulate the infrared spectra of all possible dicarbonylic products, i.e. $CH_3CH_2CH_2$**C(O)**O**C(O)**H, CH_3CH_2**C(O)**CH_2O**C(O)**H, CH_3**C(O)**CH_2CH_2O**C(O)**H, and H**C(O)**$CH_2CH_2CH_2O$**C(O)**H, (one anhydride and three esters, respectively) whose theoretical spectra are shown in Fig. 2.

Comparison of the last trace of Fig. 1 and first trace of Fig. 2 clearly shows that neither signals around 1808, 1792 cm^{-1} (C=O stretchings) nor signals at 1049 cm^{-1} (C–O–C stretchings) corresponding to the anhydride [25] are present, in accordance with the GC/MS results. On the other hand, the spectra of all the other dicarbonilyc species are similar and, consequently, the overlapping of their peaks would result in a complex spectrum similar to the one observed in the last trace of Fig. 1.

An exhaustive analysis of the behavior of the products in darkness afforded new insights about the evolution of the dicarbonylic species, suggesting that the existence of all three species would be plausible. After 30 min of photolysis, periodic monitoring of the resulting mixture was carried out during twenty-four hours. Fig. 3 shows some of the infrared spectra. Trace "A" corresponds to the spectrum of the remaining reactants and products immediately after the lamps are turned off, while traces "B" and "C," which correspond to 30 min and 24 h of

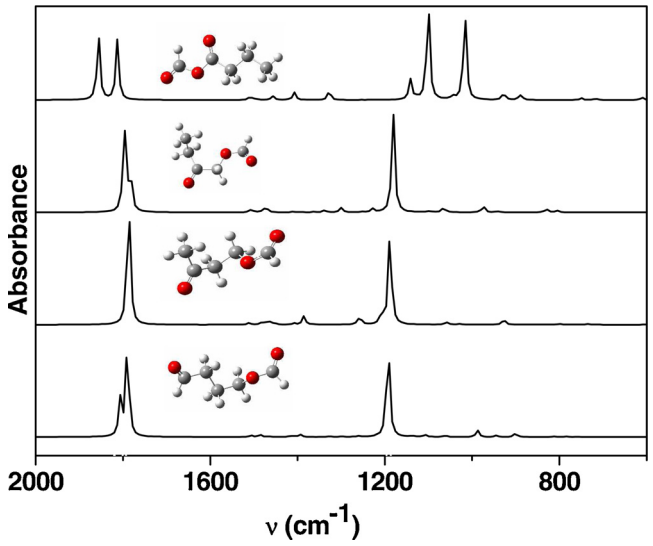

Fig. 2. From top to bottom, calculated infrared spectra of 1-, 2-, 3-, and 4-oxobutylformate.

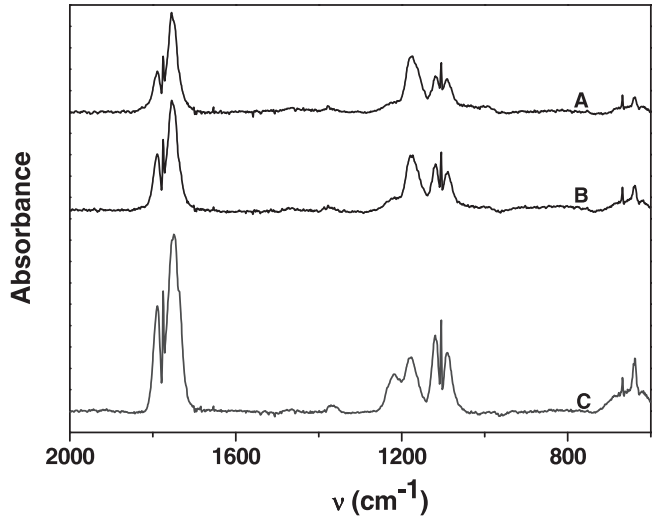

Fig. 3. Progress in reaction products while in darkness. Traces from top to bottom: "*A*", immediately after lamps are turned off; "B" 30 min later; "C" 24 h later.

darkness, undoubtedly show the increase in the concentration of formic acid during the dark period. The monitoring continued for longer periods without further variation in the concentration of formic acid.

Fig. 4 summarizes the temporal variation of formic acid. The presence of four different slopes accounting for its formation is clear, as is the fact that, after 360 min, the quantity of formic acid does not change. This could be an indication that all the unstable products have already degraded. The first slope, accounting for 19% of the reacted formate, corresponds to the formation by photo-oxidation; the second was assigned to the decomposition of $HC(O)CH_2CH_2CH_2OC(O)H$ (accounting for an additional 11%); the third and fourth slopes (which account for additional 25 and 7%) would correspond to the slow decomposition of the two experimentally measured esters, that is, $CH_3C(O)CH_2CH_2OC(O)H$ and $CH_3CH_2C(O)CH_2OC(O)H$. This assumption is based on the following facts: a) from the three dicarbonylic products, the last two species were assessed as products in our GC–MS study; b) $HC(O)CH_2CH_2CH_2OC(O)H$ should be less stable than the former ones; c) each dicarbonylic species leads to the formation of one formic acid in its own degradation path.

Fig. 5 shows the sequence of infrared spectra obtained in the photolysis of $nBF/Cl_2/NO_2/O_2$ mixtures. The first and second traces correspond to t = 0 and t = 30 min of irradiation. The third trace shows the products formed, which were obtained from the subtraction of

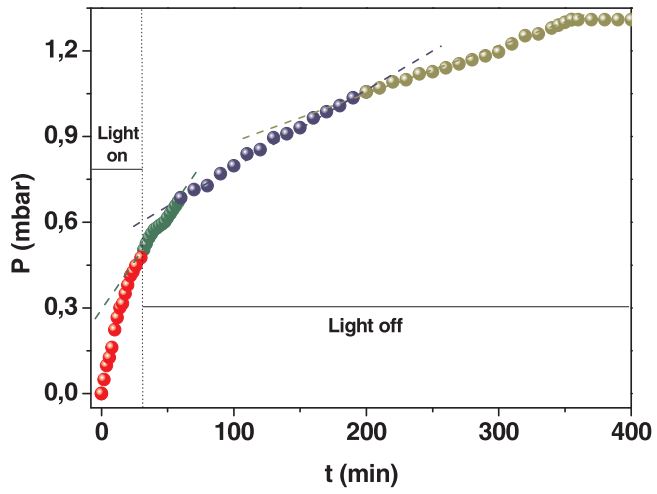

Fig. 4. Temporal variation of HC(O)OH.

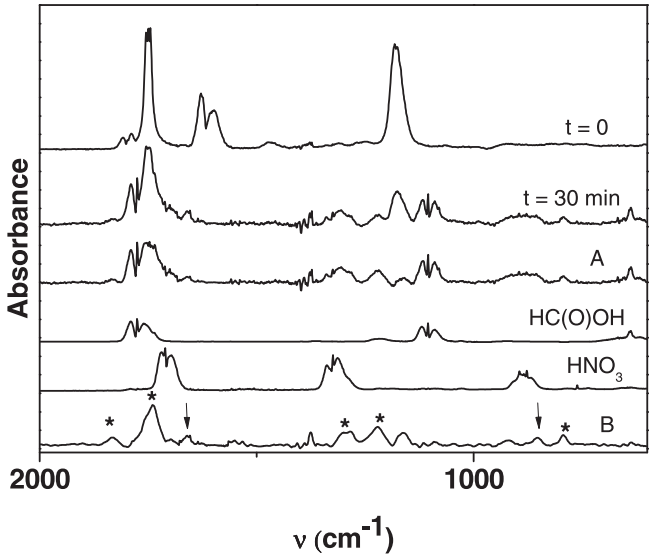

Fig. 5. Photo-oxidation in the presence of NO_2. From top to bottom: t = 0; t = 30 min photolysis; products; formic acid reference spectrum; nitric acid reference spectrum; nitrates (arrows) and peroxynitrates (asterisks) obtained from subtraction of HC(O)OH and HNO_3 to third trace.

reactants from the second trace. The fourth and fifth traces show the standard spectra of formic and nitric acids. The sixth trace, resulting from the subtraction of HC(O)OH and nitric acid to the product's trace, shows the spectrum of remaining products formed; that is, it shows the presence of signals corresponding to carbonyl bands similar to those obtained in the photo-oxidation in the absence of NO_2. Other signals corresponding to nitrates (1650 and 850 cm^{-1}) and peroxy acyl formyl nitrates, $C_xH_{2x+1}OC(O)OONO_2$, x = 1–3 (1831–1836, 1741–1748, 1219–1236 and 796–797 cm^{-1}) [18,20,26] were also observed. From the frequency of these signals and from the reaction mechanism (see below), the identity of the new peroxynitrate was assigned to peroxy butyl formyl nitrate (PBFN), $C_4H_9OC(O)OONO_2$. Its quantity was estimated assuming its cross-section similar to the average absorption cross-section of peroxyacyl formyl nitrates ($C_xH_{2x+1}OC(O)OONO_2$) reported in the literature for the peak around 1830 cm^{-1} (1.8, 1.9, 1.3 cm^2 $molecule^{-1}$; for x = 1, 2, 3 respectively) [18,20,26,27]. The formation of PBFN accounts for about (4 ± 2) % of the reacted formate.

To identify the nitrates, a photo-oxidation of a mixture of bulk quantities of nBF, Cl_2, NO_2 and oxygen was performed. The condensable products were analyzed by GC–MS spectrometry, which showed the formation of *n*-propyl and *n*-butyl nitrates. They were quantified as a single species using the average integrated band for alkyl nitrates (1635 and 1670 cm^{-1}) available in bibliography (2.5×10^{-17} cm^2 $molecule^{-1}$) [28] and account for (11 ± 1) % of the formate reacted.

Aldehydes formation was certified by the ^1H NMR spectra of the mixtures of products. Propanal and butanal were identified, based on the shift (δ −ppm−) for the hydrogen of the carbonyl group, at 9.79 and 9.76. An upper limit of propanal formation (15 ± 2%) was estimated by the subtraction of a reference spectrum to the products spectra, until no negative peaks were observed in the resulting traces.

3.2. Reaction mechanism

The rapid photo-oxidation of nBF initiated by chlorine atoms (whose rate coefficients range from 1.4 to 1.1×10^{-10} cm^3 $molec^{-1}$ s^{-1}) [13,15] leads to the abstraction of hydrogen atoms in five different sites of the molecule to form radicals (Reactions (1a)–(1e)):

$CH_3CH_2CH_2CH_2OC(O)H + Cl\cdot \rightarrow CH_3CH_2CH_2CH_2OC(O)\cdot + HCl$ (1a)

$CH_3CH_2CH_2CH_2OC(O)H + Cl\cdot \rightarrow CH_3CH_2CH_2CH\cdot OC(O)H + HCl$ (1b)

$CH_3CH_2CH_2CH_2OC(O)H + Cl\cdot \rightarrow CH_3CH_2CH\cdot CH_2OC(O)H + HCl$ (1c)

$CH_3CH_2CH_2CH_2OC(O)H + Cl\cdot \rightarrow CH_3CH\cdot CH_2CH_2OC(O)H + HCl$ (1d)

$CH_3CH_2CH_2CH_2OC(O)H + Cl\cdot \rightarrow CH_2\cdot CH_2CH_2CH_2OC(O)H + HCl$ (1e)

All these radicals react with molecular oxygen to form peroxy radicals (ROO·) that could either recombine, react with other peroxy radicals or chlorine atoms to form RO· radicals or react with nitrogen dioxide to form the corresponding peroxynitrate $RC(O)OONO_2$. According to the structure of the RO· radicals, different reaction paths are opened that will be described in detail below.

3.2.1. Via 1a

The $CH_3CH_2CH_2CH_2OC(O)\cdot$ radical in the presence of O_2 leads to the formation of the peroxy radical $CH_3CH_2CH_2CH_2OC(O)OO\cdot$ which, in the presence of NO_2, forms the PBFN. This peroxynitrate should be stable on account of the stability of the $C_xH_{2x+1}OC(O)OONO_2$ family. Members of this family have been observed in the photolysis of methyl formate [18], ethyl formate [19,26,27] and propyl formate [20] and have been fully characterized by infrared spectroscopy. However, the thermal equilibrium that they establish provides peroxy radicals $CH_3CH_2CH_2CH_2OC(O)OO\cdot$ which could react with nitrogen monoxide (product of the photochemical rupture of NO_2) to form $CH_3CH_2CH_2CH_2OC(O)O\cdot$ radicals which, in turn, lead to the formation of carbon dioxide and $CH_3CH_2CH_2CH_2O\cdot$ (Reaction (2)):

$CH_3CH_2CH_2CH_2OC(O)O\cdot \rightarrow CH_3CH_2CH_2CH_2O\cdot + CO_2$ (2)

and subsequently continue to:

$CH_3CH_2CH_2CH_2O\cdot + O_2 \rightarrow CH_3CH_2CH_2C(O)H + HO_2\cdot$ (3)

$CH_3CH_2CH_2CH_2O\cdot + NO_2 \rightarrow CH_3CH_2CH_2CH_2ONO_2$ (4)

Both $CH_3CH_2CH_2CH_2ONO_2$ (butyl nitrate) and butanal were observed as photolysis products given the fact that both reactions effectively compete on account of their rate coefficients ($k_3 = 9.5 \times 10^{-12}$, $k_4 = 3.3 \times 10^{-11}\,cm^3\,molec^{-1}\,s^{-1}$) [29,30] and the pressures used ($p_{O2} = 1000$ mbar; $p_{NO2} = 2$ mbar), giving a ratio v_4/v_3 of ≈ 8.

3.2.2. Via 1b

The original radical formed in Reaction (1b) leads (via reaction with O_2 and NO or Cl atoms) to the radical $CH_3CH_2CH_2CHO\cdot OC(O)H$ that could, a priori, react either via α-ester rearrangement (Reaction (5)), with molecular oxygen (Reaction (6)) or decompose (Reaction (7)):

$CH_3CH_2CH_2CHO\cdot OC(O)H \rightarrow CH_3CH_2CH_2C(O)\cdot + HC(O)OH$ (5)

$CH_3CH_2CH_2CHO\cdot OC(O)H + O_2 \rightarrow CH_3CH_2CH_2C(O)OC(O)H + HO_2\cdot$ (6)

$CH_3CH_2CH_2CHO\cdot OC(O)H \rightarrow CH_3CH_2CH_2C(O)H + HC(O)O\cdot$ (7)

According to the reactions proposed for similar radicals, $CH_3CH_2CHO\cdot OC(O)H$ [20], $CH_3C(O)OCHO\cdot CH_3$, and $CH_3C(O)OCHO\cdot CH_2CH_3$ [31], the main path should be the α-ester rearrangement followed by a reaction with molecular oxygen. One way to prove it was the calculation of the relative energies for Reactions (5)–(7) using GAUSSIAN 09: the values obtained were 16, 92, and 60 kJ/mol, respectively, showing that rearrangement is the only path available for this radical. This is also accompanied (see mechanism) by the formation of either propanal and carbon dioxide, or peroxy *n*-propyl nitrate ($CH_3CH_2CH_2C(O)OONO_2$) and *n*-propyl nitrate $CH_3CH_2CH_2ONO_2$ when nitrogen dioxide is present. Total nitrates (butyl- and propyl-) formed by *vias* a and b account (11 ± 1) % of the formate reacted.

3.2.3. Via 1c

The radical resulting from Reaction (1c), $CH_3CH_2CHO\cdot CH_2OC(O)H$, continues to give:

$CH_3CH_2CHO\cdot CH_2OC(O)H + O_2 \rightarrow CH_3CH_2C(O)CH_2OC(O)H$ (8)

$CH_3CH_2CHO\cdot CH_2OC(O)H \rightarrow CH_3CH_2C(O)H + \cdot CH_2OC(O)H$ (9a)

$CH_3CH_2CHO\cdot CH_2OC(O)H \rightarrow CH_3CH_2\cdot + HC(O)CH_2OC(O)H$ (9b)

$CH_3CH_2CHO\cdot CH_2OC(O)H \rightarrow CH_3CH_2CHOHCH_2OC(O)\cdot$ (10)

The formation of 2-oxobutil formate ($CH_3CH_2C(O)CH_2OC(O)H$) observed by GC–MS spectrometry corroborates the occurrence of Reaction (8). However, decomposition could also be feasible for these radicals, as was proposed for the $CH_3CHO\cdot CH_2OC(O)CH_3$ radical in the photo-oxidation of *n*-propyl acetates [31]. Nevertheless, in our system, there is no evidence that Reaction (9b) would occur (on account of the absence of $CH_3C(O)H$ formation that should be expected if $CH_3CH_2\cdot$ radicals were present). Besides, neither CO nor HC(O)OC(O)H formations from reactions subsequent to (9a) (Reactions (11)–(15)) were observed within our experimental errors:

$\cdot CH_2OC(O)H + O_2 \rightarrow \cdot OOCH_2OC(O)H$ (11)

$\cdot OOCH_2OC(O)H + RO_2\cdot \rightarrow 2\ \cdot OCH_2OC(O)H + O_2$ (12)

$\cdot OCH_2OC(O)H + O_2 \rightarrow HC(O)OC(O)H$ (13)

$\cdot OCH_2OC(O)H \rightarrow HC(O)\cdot + HC(O)OH$ (14)

$HC(O)\cdot + O_2 \rightarrow CO + HO_2\cdot$ (15)

However, formic acid, which is a measured product, could have appeared from Reaction (14), making difficult to conclusively discard the occurrence of (9a). Indeed, we could neither assess its occurrence, since formic acid is also formed by via (1b) – Reaction (5) – nor discard it on account of the lack of CO and HC(O)OC(O)H. The total formation of HC(O)OH, coming either from via (1b), or eventually via (1c), accounts for about (19 ± 1) % of the reacted formate.

3.2.4. Via 1d

The radical resulting from Reaction (1d), $CH_3CHO\cdot CH_2CH_2OC(O)H$, could react with oxygen (Reaction (16)) or decompose (Reactions (17a) and (17b)):

$CH_3CHO\cdot CH_2CH_2OC(O)H + O_2 \rightarrow CH_3C(O)CH_2CH_2OC(O)H$ (16)

$CH_3CHO\cdot CH_2CH_2OC(O)H \rightarrow CH_3C(O)H + \cdot CH_2CH_2OC(O)H$ (17a)

$CH_3CHO\cdot CH_2CH_2OC(O)H \rightarrow CH_3\cdot + HC(O)CH_2CH_2OC(O)H$ (17b)

The only product unambiguously identified was 3-oxobutil formate ($CH_3C(O)CH_2CH_2OC(O)H$). Therefore, Reaction (17a) was discarded (acetaldehyde was not observed by GC/MS), as well as Reaction (17b) ($CH_3\cdot$ radicals should lead to formaldehyde or eventually carbon monoxide, if further degraded during the experiment. Neither of them were observed). The preceding discussion suggests that the main path for the $CH_3CHO\cdot CH_2CH_2OC(O)H$ radical is the reaction with molecular oxygen. The formation of $CH_3C(O)CH_2CH_2OC(O)H$ (via 1c, Scheme 1) and $CH_3CH_2C(O)CH_2OC(O)H$ (via 1d, Scheme 1) accounts for an extra 32% of reacted formate.

3.2.5. Via 1e

The last oxy radical, $CH_2O\cdot CH_2CH_2CH_2OC(O)H$ formed from Reaction (1e), could result in (Reactions (18)–(20)):

$CH_2O\cdot CH_2CH_2CH_2OC(O)H + O_2 \rightarrow HC(O)CH_2CH_2CH_2OC(O)H$ (18)

$CH_2O\cdot CH_2CH_2CH_2OC(O)H \rightarrow CH_2(OH)CH_2CH_2CH\cdot OC(O)H$ (19)

$CH_2O\cdot CH_2CH_2CH_2OC(O)H \rightarrow CH_2O + \cdot CH_2CH_2CH_2OC(O)H$ (20)

The formation of 4-oxobutyl formate ($HC(O)CH_2CH_2CH_2OC(O)H$)

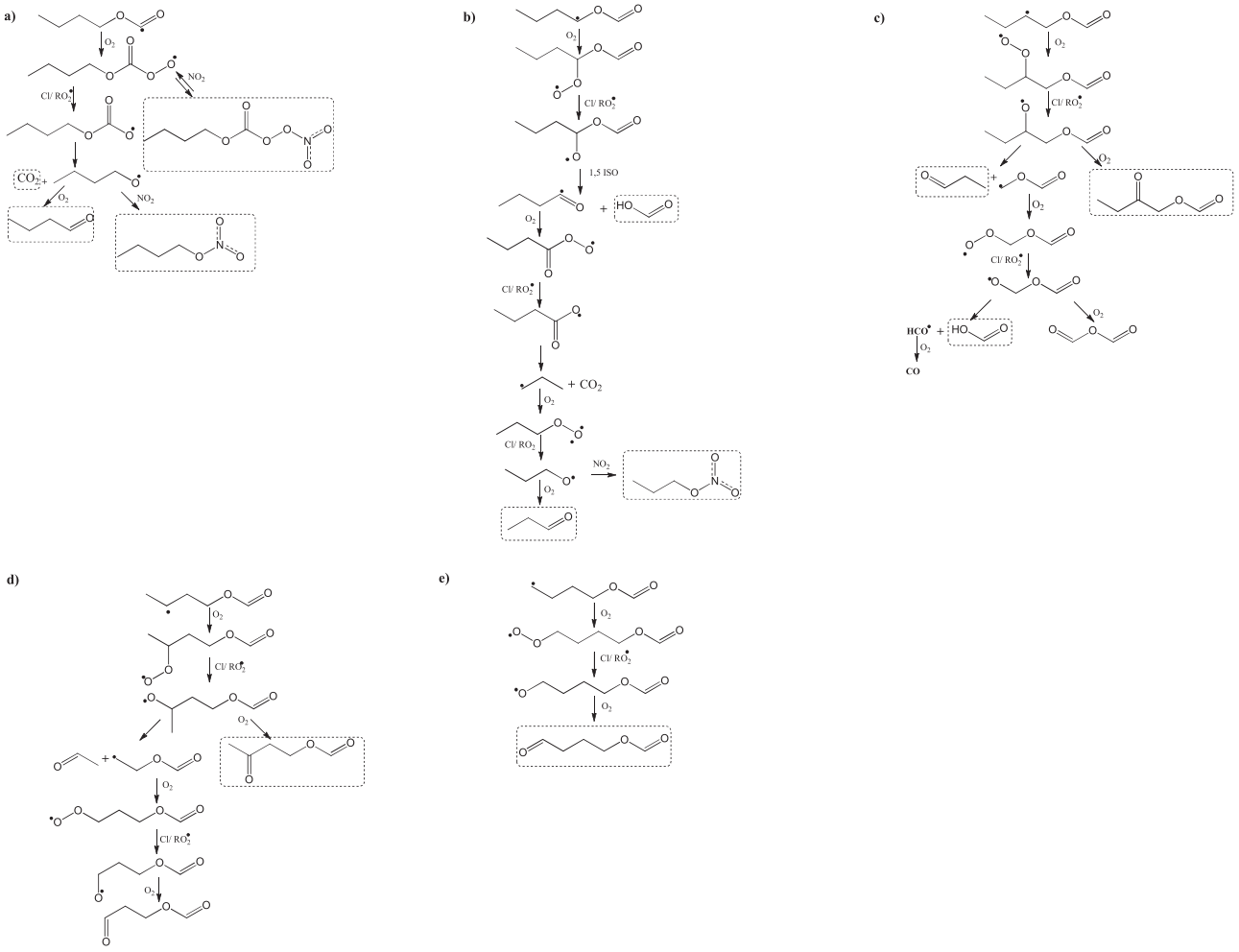

Scheme 1. Reaction mechanism of *n*-butyl formate. Subset "a" to "e" presents the sequence of reactions initiated by the attack of chlorine atoms to the different hydrogen atoms. The compounds identified are enclosed in a box.

(Reaction (18)) is observed by GC/MS and accounts for about (6 ± 1) % of the reacted formate. This result is in concordance with the observations of Picquet et al. [31] in the photo-oxidation of *n*-propyl acetate, where the main path for $CH_3C(O)OCH_2CH_2CH_2O\cdot$ is the reaction with O_2 [32].

3.3. Some comments about SARs (structure-activity relationships)

In order to check the reliability of our experimental results with regards to the relative amounts of products formed, the SAR method was used. Three different approaches were performed to calculate the relative weigh of the attack of chlorine atoms on every abstractable hydrogen of the molecule, namely:

i Using the values reported by Notario et al. [13] for the substituents bonded to the methyl, methylene, and methanetriyl groups: F(−OC(O)) = 0.05; F(−CH_2−O−C(O)) = 0.28.

ii Using the rate coefficients suggested by Calvert et al. [9] for *n*-propyl-, isopropyl-, and *tert*-butyl formate, selected because of their values (4,6; 1,76 and 1.45×10^{-11} $cm^3\,molec^{-1}\,s^{-1}$, respectively) and proposing a set of three equations with three variables. Within this system, k_a which corresponds to the attack at the hydrogen of the carbonyl group, was assumed independent on the chain length of the carbon skeleton. The parameters F(−OC(O)) and F(−CH_2−O−C(O)) obtained take the values listed in Table 1.

iii Taking the experimental data by Pimentel et al. [33] for isopropyl (30, 50, and 20% for the hydrogen atom of the carbonyl, methyl, and methanetriyl groups) and *tert*-butyl (49 and 51% for carbonyl and methyl groups) formates. From these data k_a, F(−OC(O)), F(−CH_2−O−C(O)), F(⅄C−O−C(O)) were calculated.

Table 1 summarizes the results with these three approaches. In the calculation, the values of $k_{PRIM} = 3.32 \times 10^{-11}$, $k_{SEC} = 8.34 \times 10^{-11}$, $k_{TERT} = 6.09 \times 10^{-11}$ $cm^3\,molec^{-1}\,s^{-1}$ and F(−CH_3) = 1.00, F(−CH_2−) = 0.79 taken from Aschmann et al. [34] were used. Factor groups F(−CH_2−O−C(O)), F(> CH−O−C(O)), F(⅄C−O−C(O)) were considered equal. As can be seen, the data obtained using methods II and III for k_a and F groups show an acceptable match. The calculation of the mean value for these variables gives the following results: $k_a = 5.7 \times 10^{-12}$ $cm^3\,molec^{-1}\,s^{-1}$, F(−OC(O)) = 0.12, F(−CH_2−O−C(O)) = F(> CH−O−C(O)) = F(⅄C−O−C(O)) = 0.075. Although the values do not exactly coincide with those obtained by Notario et al. [13] for the whole family of formates, they are not so different either and are more in agreement with the experimental results. According to them, the rate coefficient of chlorine atoms with nBF (k_{nBF}) gives 11.1×10^{-12} $cm^3\,molec^{-1}\,s^{-1}$, in excellent agreement with the rate coefficient suggested by Calvert et al. [9]. From this value and k_a, the relative percentage of chlorine atom attack to the hydrogen of the carbonylic carbon is around 5%, in excellent agreement with the experimental percentage of $CH_3CH_2CH_2CH_2OC(O)OONO_2$ (4 ± 2%) formed via "a" in Scheme 1. In a similar way, the value of k_a for *n*-propyl formate gives a theoretical percentage (12%), in agreement with the experimental one obtained by Vila et al. [20] for the formation of $CH_3CH_2CH_2OC(O)OONO_2$ (around 10%). With our values determined

Table 1
SAR parameters.

Method used	*Molecules*	$k_a \times 10^{12}$*	F(−OC(O))	F(−CH_2−O−C(O)) F(> CH−O−C(O))	F(⊥C−O−C(O))	Refs.
I	formates	–	0.05	0.28		[13]
II	isopropyl, *tert*-butyl and *n*-propyl formates	4.8	0.10	0.097		This work
III	isopropyl	5.3	0.14	0.053		This work
	tert-butyl	7.1	–	0.074		This work

* In units of $cm^3\,molec^{-1}\,s^{-1}$.

for k_a, F(−OC(O)) and F(−CH_2−O−C(O)) and the values corresponding to F(−CH_2−) = 0.79 [34], the relative percentage of the attack of chlorine atoms on the different carbons are 5.1, 7.1, 4.5, 59.7, and 23.4% respectively for vias a–e.

Unfortunately, experimental determination of the relative percentage of each *via* is not simple since some products are formed in more than one way and, consequently, a comparison with the data obtained from SAR is not straightforward. V*ia* a is, however, an exception because its contribution can be established from the amount of PBFN (4%), in agreement with the percentage obtained from the SAR method (5%). As can be seen in Scheme 1, formic acid (19 ± 2%) and propanal (15 ± 2%) come both through vias "b" and "c" and having the same (1:1) ratio. Nevertheless, both percentages (within experimental errors) are in agreement with a mean value of 17%, representing the formation of both products. Considering the fact that $CH_3CH_2C(O)CH_2OC(O)H$ is also formed from via c (7 ± 2%), the total experimental percentage (24%) does not match the SAR value (12%). However, that low relative percentage speaks for the deactivating effect of the C(O)O− group both in α- and β- positions.

On the other hand, the formation of $CH_3C(O)CH_2CH_2OC(O)H$ (25 ± 2) % and $HC(O)CH_2CH_2CH_2OC(O)H$ (11 ± 2) % (coming from vias d and e, respectively) suggests that the attack on the methyl group occurs to a minor extent as on the adjacent methylene group. The SAR method gives 59 and 22% for the attack on these groups. However, these values disagree considerably with the experimental ones, and only the relative percentage of these vias are in concordance.

4. Conclusion

Our paper extends the study on the series of formates for the determination of reaction mechanisms in the presence and absence of nitrogen dioxide. Its photo-oxidation mainly leads to the formation of aldehydes, formic acid, and dicarbonylic products. In the presence of high NO_2 concentrations, a new peroxynitrate ($CH_3CH_2CH_2CH_2OC(O)OONO_2$), as well as nitrates ($CH_3CH_2CH_2CH_2ONO_2$, $CH_3CH_2CH_2ONO_2$) are formed.

The comparison of the yield of $CH_3CH_2CH_2CH_2OC(O)OONO_2$ (4%) with the yield of $CH_3CH_2CH_2OC(O)OONO_2$ (~10%) from the photo-oxidation of *n*-propyl formate, shows that the attack on the hydrogen of the carbonyl group for formates of relatively long carbonated chains is lesser than the attack to other hydrogen atoms. Instead, our SAR values agree with those experimental values.

The results also allow to draw conclusions on the deactivating effect of the carbonyl group over the α- and β- positions. The attack of chlorine atoms to form HC(O)OC·HR radicals in *n*-propyl formate is around 15% while it is only 7% in *n*-butyl formate.

Acknowledgments

Financial support from SECYT-Universidad Nacional de Córdoba, ANPCyT, and CONICET is gratefully acknowledged. JAV acknowledges the fellowship he holds from CONICET.

References

[1] T. Simpson, V. Bikoba, E.J. Mitcham, Effects of ethyl formate on fruit quality and target pest mortality for harvested strawberries, Postharvest Biol. Technol. 34 (2004) 313–319.
[2] T. Simpson, V. Bikoba, C. Tipping, E.J. Mitcham, Ethyl formate as a postharvest fumigant for selected pest of table grapes, J. Econ. Entomol. 100 (2007) 1084–1090.
[3] J.M. Desmarchelier, Ethyl formate and formic acid: occurence and environmental fate, Postharvest News Inf. 10 (1999) 7–12.
[4] J.M. Desmarchelier, F.M. Johnston, V. Le Trang, Ethyl formate formic acid and etanol in air, wheat, barley and sultanas: analysis of natural levels and fumigant residues, Pest. Sci. 55 (1999) 815–824.
[5] M. Agarwal, Ethyl Formate: a potential disinfestation treatment for eucalyptus weevil (gonipterus platensis) (coleoptera: curculionidae) in apples, J. Econ. Entomol. 108 (2015) 2566–2571.
[6] J. Eberhard, C. Müller, D.W. Stocker, J.A. Kerr, The photo-oxidation of diethyl ether in smog chamber experiments simulating tropospheric conditions. Products studies and proposed mechanism, Int. J. Chem. Kinet. 25 (1993) 639–649.
[7] T.J. Wallington, S.M. Japar, Atmospheric chemistry of diethyl ether and ethyl *tert*-butyl ether, Environ. Sci. Technol. 25 (1991) 410–415.
[8] E.M. Yahia, Apple flavor, Hortic. Rev. 16 (2010) 197–273.
[9] J.G. Calvert, A. Mellouki, J.J. Orlando, M.J. Pilling, T.J. Wallington, The Mechanism of Atmospheric Oxidation of the Oxygenates, Oxford University Press, 2011.
[10] S. Langer, E. Ljungström, I. Wängberg, Rates of reaction between the nitrate radical and some aliphatic esters, J. Chem. Soc. Faraday Trans. 89 (1993) 425–431.
[11] R. Atkinson, W.P.L. Carter, Kinetics and mechanisms of the gas-phase reactions of ozone with organic compounds under atmospheric conditions, Chem. Rev. 84 (1989) 437–470.
[12] S. LeCalve, G. LeBras, A. Mellouki, Temperature dependence for the rate coefficients of the reactions of the OH radicals with a series of formates, J. Phys. Chem. A 101 (1997) 5489–5493.
[13] A. Notario, G. Le Bras, A. Mellouki, Absolute rate constants for the reactions of Cl atoms with a series of esters, J. Phys. Chem. A 102 (1998) 3112–3117.
[14] S.R. Sellevåg, C.J. Nielsen, Kinetic study of the reactions CH_2ClCH_2Cl + OH, $CH_3C(O)CH_3$ + Cl and $HC(O)OCH_2CH_3$ + Cl by the relative rate method, Asian Chem. Lett. 7 (2003) 15–20.
[15] T.J. Wallington, M.D. Hurley, A. Haryanto, Kinetics of the gas phase reactions of chlorine atoms with a series of formates, Chem. Phys. Lett. 432 (2006) 57–61.
[16] T. Ide, E. Iwasaki, Y. Matsumi, J. Xing, K. Takahashi, T.J. Wallington, Pulsed laser photolysis vacuum UV laser-induced fluorescence kinetic study of the reactions of $Cl(^2P_{3/2})$ atoms with ethyl formate *n*-propyl formate, and *n*-butyl formate, Chem. Phys. Lett. 467 (2008) 70–73.
[17] Y.J. Zhang, P. Liang, Z.H. Jiang, M. Cazaunau, V. Daële, Y.J. Mu, A. Mellouki, Reactions of OH and Cl with isopropyl formate isobutyl formate, *n*-propyl isobutyrate and isopropyl isobutyrate, Chem. Phys. Lett. 602 (2014) 68–74.
[18] T.J. Wallington, M.D. Hurley, T. Maurer, I. Barnes, K.H. Becker, G.S. Tyndall, J.J. Orlando, A.S. Pimentel, M. Bilde, Atmospheric oxidation mechanism of methyl formate, J. Phys. Chem. A 105 (2001) 5146–5154.
[19] F.E. Malanca, J.C. Fraire, G.A. Argüello, Kinetics and reaction mechanism in the oxidation of ethyl formate in the presence of NO_2, J. Photochem. Photobiol. A: Chem. 204 (2009) 75–81.
[20] J.A. Vila, F.E. Malanca, G.A. Argüello, Photolysis of *n*-propyl formate in the presence of O_2 and NO_2: peroxyformyl propyl nitrate $CH_3CH_2CH_2OC(O)OONO_2$ synthesis and characterization, J. Phys. Chem. A 120 (2016) 241–246.
[21] M.J. Frisch, G.W. Trucks, H.B. Schlegel, G.E. Scuseria, M.A. Robb, J.R. Cheeseman, G. Scalmani, V. Barone, B. Mennucci, G.A. Petersson, H. Nakatsuji, M. Caricato, X. Li, H.P. Hratchian, A.F. Izmaylov, J. Bloino, G. Zheng, J.L. Sonnenberg, M. Hada, M. Ehara, K. Toyota, R. Fukuda, J. Hasegawa, M. Ishida, T. Nakajima, Y. Honda, O. Kitao, H. Nakai, T. Vreven, J.A. Montgomery Jr., J.E. Peralta, F. Ogliaro, M. Bearpark, J.J. Heyd, E. Brothers, K.N. Kudin, V.N. Staroverov, R. Kovayashi, J. Normand, K. Raghavachari, A. Rendell, J.C. Burant, S.S. Iyendar, J. Tomasi, M. Cossi, N. Rega, J.M. Millam, M. Klene, J.E. Knox, J.B. Cross, V. Bakken, C. Adamo, J. Jaramillo, R. Gomperts, R.E. Stramann, O. Yazyev, A.J. Austin, R. Cammi, C. Pomelli, J.W. Ochterski, R.L. Martin, K. Morokuma, V.G. Zakrzewski, G. Voth, P. Salvador, J.J. Dannenberg, S. Dapprich, A.D. Daniels, Ö. Farkas, J.B. Foresman, J.V. Ortiz, J. Cioslowski, D.J. Fox, Gaussian 09, Revision E01, Gaussian, Inc., Walligford, CT, 2009.
[22] G.N. Rimondino, D.P. Henao, W. Peláez, G.A. Argüello, F.E. Malanca, Photo-oxidation of dimethyl malonate Initiated by chlorine atoms in gas phase: kinetics and mechanism, J. Phys. Chem. A 121 (2017) 8577–8582.
[23] D.P. Henao Arboleda, G.A. Argüello, F.E. Malanca, Chlorine initiated

photooxidation of $(CH_3)_3CC(O)H$ in the presence of NO2 and photolysis at 254 nm. Synthesis and thermal stability of $(CH_3)_3CC(O)OONO_2$, J. Photochem. Photobiol. A: Chem. 299 (2015) 62–66.
[24] M.P. Badenes, C.J. Cobos, Quantum chemical study of the atmospheric $C_2H_5C(O)OONO_2$ (PPN) molecule and of the $C_2H_5C(O)OO$ and $C_2H_5C(O)O$ radicals, J. Mol. Struct.: Theochem. 856 (2008) 59–70.
[25] G. Wu, S. Shlykov, C. Van Alsenoy, H.J. Geise, E. Sluyts, B.J. Van der Veken, Formic acetic anhydride in the gas phase studied by electron diffraction and infrared spectroscopy, supplemented with ab-Initio calculations of geometries and force fields, J. Phys. Chem. 100 (1996) 11620–11629.
[26] A.G. Bossolasco, F.E. Malanca, G.A. Argüello, Peroxy ethoxy formyl nitrate $CH_3CH_2OC(O)OONO_2$, spectroscopic and thermal characterization, J. Photochem. Photobiol. A: Chem. 221 (2011) 58–63.
[27] J.J. Orlando, G.S. Tyndall, The atmospheric oxidation of ethyl formate and ethyl acetate over range of temperatures and oxygen partial pressures, Int. J. Chem. Kinet. 42 (2010) 397–413.
[28] S.M. Aschmann, P. Martin, E.C. Tuazon, J. Arey, R. Atkinson, Kinetic and product studies of the reactions of selected glycol ethers with OH radicals, Environ. Sci. Technol. 35 (2001) 4080–4088.
[29] R. Atkinson, D.L. Baulch, R.A. Cox, J.N. Crowley, R.F. Hampson Jr., J.A. Kerr, M.J. Rossi, J. Troe, Summary of Evaluated Kinetic and Photochemical Data for Atmospheric Chemistry, IUPAC Subcommittee on Gas Kinetic Data Evaluation for Atmospheric Chemistry Web Version, 2001, 2018.
[30] Ch. Lotz, R. Zellner, Fluorescence excitation spectrum of the 2-butoxyl radical and kinetics of its reactions with NO and NO_2, Phys. Chem. Chem. Phys. 3 (2001) 2607–2613.
[31] B. Picquet-Varrault, J.-F. Doussin, R. Durand-Jolibois, P. Carlier, FTIR spectroscopic study of the OH-induced oxidation of two linear acetates: ethyl and *n*-propyl acetates, Phys. Chem. Chem. Phys. 3 (2001) 2595–2606.
[32] J.J. Orlando, G.S. Tyndall, T.J. Wallington, The atmospheric chemistry of alkoxy radicals, Chem. Rev. 103 (2003) 4657–4689.
[33] A.S. Pimentel, G.S. Tyndall, J.J. Orlando, M.D. Hurley, T.J. Wallington, M.P.S. Andersen, P. Marshall, T.S. Dibble, Atmospheric chemistry of isopropyl formate and tert-butyl formate, Int. J. Chem. Kinet. 42 (2010) 479–498.
[34] S.M. Aschmann, R. Atkinson, Rate constants for the gas-phase reactions of alkanes with Cl atoms at 296 ± 2 K, Int. J. Chem. Kinet. 27 (1995) 613–622.